

Ferromagnetic Kondo lattice model with Rashba coupling: effects of antiferromagnetic coupling between localized spins.

Giovanly A. Meza and José A. Riera

Instituto de Física Rosario y Departamento de Física,
Universidad Nacional de Rosario, Rosario, Argentina

E-mail: riera@ifir-conicet.gov.ar

Abstract. Motivated by emergent phenomena at oxide surfaces and interfaces involving transition metal oxides, we examine the ferromagnetic Kondo lattice model (FKLM) in the presence of a Rashba spin-orbit coupling (RSOC) at zero temperature using numerical techniques. We find that the main effect of the RSOC is the destruction of the ferromagnetic state present in the FKLM at low electron fillings, with the consequent suppression of conductivity. In addition, near half-filling the RSOC leads to a departure of the antiferromagnetic state of the FKLM with a consequent reduction to the intrinsic tendency to electronic phase separation. A similar behavior is observed at very low electron density in the presence of an antiferromagnetic coupling between localized spins.

1. Introduction

So-called emergent electrodynamics phenomena at the interface between strongly correlated materials, and particularly transition metal oxides (TMO), or at the surface of such materials, have been revealed by a number of theoretical and experimental studies [1]. In essence, this exciting new physical phenomena is induced by the breaking of the inversion symmetry at the interface (or surface) itself. As a result of this broken symmetry, and due to relativistic arguments, it appears the so-called Rashba effect [2, 3, 4], which describes various momentum-dependent spin-splitting processes, including spin currents and the spin-Hall effect [5, 6]. As emphasized in a rather extensive literature, the RSOC leads to new applications in spintronics [7] since in an appropriate device this coupling can also be tuned by an external gate voltage.

Various types of interfaces between TMOs where RSOC is present have been studied, mostly involving SrTiO_3 [8, 9], but also $\text{LaMnO}_3/\text{SrMnO}_3$ interfaces [10] have been considered. The contribution of gate tunable RSOC in addition to the in-plane RSOC of broken symmetry origin, has been measured in $\text{LaAlO}_3/\text{SrTiO}_3$ interfaces [9]. Experimental indications of RSOC have also been reported at surfaces in SrTiO_3 [11].

The microscopic description of several transition metal oxides and heavy fermions is achieved through generalizations of the ferromagnetic Kondo lattice model [12, 13, 14, 15, 16] (FKLM) also called the double exchange model particularly when the Hund coupling is much larger than the hopping integral. For a large Hund coupling, it is known that there is a metallic ferromagnetic (FM) phase up to a filling $\nu \sim 0.8$, followed by a tendency towards an antiferromagnetic (AFM) state with semiconducting or insulating properties [17, 18, 19, 20]. Another important issue



that has been thoroughly discussed in the context of manganites is the presence of an instability towards phase separation (PS) [16, 19], which will be also examined here.

In this work we will continue the study of the RSOC effects on the magnetic and transport properties in the single-orbital 2D FKLM, which was started in Ref. [21]. Of course, a more realistic model would take into account the fact that in TMOs with perovskite structure, the originally five-fold degenerate 3d orbitals are split into three-fold degenerate t_{2g} orbitals xy, yz, zx and two-fold degenerate e_g orbitals $x^2 - y^2, 3z^2 - r^2$. There is additional complexity at the interface such as dynamical transfer of electrons from the bulk and location of the interface layer [22, 23, 24]. By starting with the study of a single orbital model, we follow the program which has been pursued for example in the study of manganites and on the competition between the Rashba and Hubbard couplings [25]. In the present work we take a step towards a more realistic model by including an antiferromagnetic coupling between localized spins.

2. Model and method

The Rashba-FKLM for a single delocalized orbital coupled to classical localized spins is defined by the Hamiltonian $H_{10} = H_0 + H_{int}$, where:

$$\begin{aligned} H_0 &= -t_0 \sum_{\langle l,m \rangle, \sigma} (c_{l\sigma}^\dagger c_{m\sigma} + H.c.) + \lambda_{SO} \sum_l [c_{l+x\downarrow}^\dagger c_{l\uparrow} \\ &\quad - c_{l+x\uparrow}^\dagger c_{l\downarrow} + i(c_{l+y\downarrow}^\dagger c_{l\uparrow} + c_{l+y\uparrow}^\dagger c_{l\downarrow}) + H.c.] \\ H_{int} &= -J_H \sum_l \mathbf{S}_l \cdot \mathbf{s}_l + U \sum_l n_{l\uparrow} n_{l\downarrow} + J \sum_{\langle l,m \rangle} \mathbf{S}_l \cdot \mathbf{S}_m \end{aligned} \quad (1)$$

The first term in the noninteracting part H_0 , is the usual hopping term, $H_{0,hop}$, and the second one corresponds to the RSOC, $H_{0,SO}$, assuming a square lattice in the xy plane (z is the spin quantization axis) [26]. The first term in the interacting part of the Hamiltonian H_{int} is the ferromagnetic Hund term, H_H , between localized \mathbf{S}_l and conduction electron \mathbf{s}_l spins. The second term is the Hubbard repulsion between conduction electrons, H_U , and the last one corresponds to the AFM exchange Hamiltonian between localized spins, H_J . We set $U = 0$, which is a reasonable assumption at least for SrTiO₃ [22, 23]. We normalize the hopping and RSOC parameters as $t_0^2 + \lambda_{SO}^2 = 1$ whose square root will be henceforth adopted as the unit of energy. The solely parameters left are then the ratio λ_{SO}/t_0 , J , and the electron filling $\nu \equiv N_e/N$ ($N \equiv L \times L$).

In this work, we will employ a Monte Carlo technique that is based on the assumption that the localized spins are described by classical continuum spins $\mathbf{S}_l = (S, \theta_l, \phi_l)$ in spherical coordinates [16, 17]. In the present study, we resort to the so-called perturbative Monte Carlo (PMC) [27, 28], in which the full Hamiltonian is only diagonalized after a sweep on the whole lattice. Since in this work we limit ourselves to study zero temperature properties, the Monte Carlo simulation is reduced to a simple optimization procedure, the so-called simulated annealed optimization, in which a Boltzmann weight is used with a parameter that plays the role of “temperature”. Further details can be found in Ref. [21].

3. Results

3.1. Magnetic properties

In the pure FKLM, various types of magnetic order have been detected in the J_H -density phase diagram in 2D, and this variety is even richer in the presence of an AFM interaction between localized spins J [17, 18]. As we show in this Subsection, this is also the case when λ_{SO} is turned on, even at a fixed $J_H = 10$. To understand the magnetic behavior, the spin-spin correlations between localized spins, $C(\mathbf{r}) = \langle \mathbf{S}_\mathbf{r} \cdot \mathbf{S}_\mathbf{0} \rangle$ ($\mathbf{0}$ is the reference site), and their Fourier transform leading to the static magnetic structure function $\chi(\mathbf{k})$, have been computed.

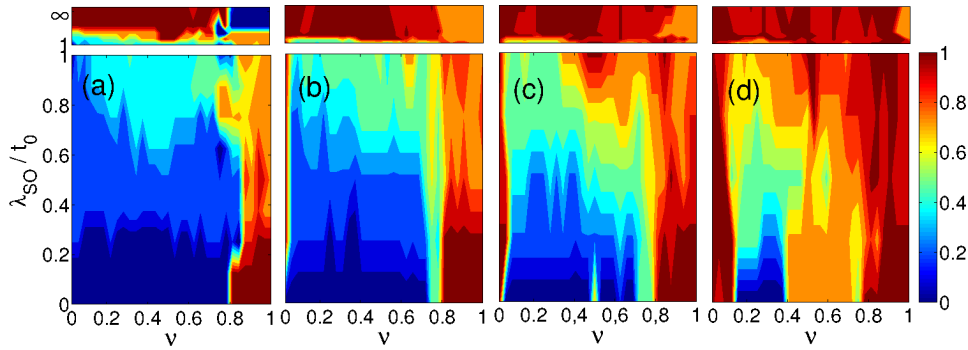


Figure 1. Magnetic phase diagram in the electron density- λ_{SO}/t_0 plane determined from the modulus of the peak of the magnetic structure factor, where dark blue corresponds to FM order ($|\mathbf{k}_{peak}| = 0$) and dark red to AFM order ($|\mathbf{k}_{peak}| = 1$). From left to right, $J = 0, 0.01, 0.025$, and 0.05 . Results for the 8×8 cluster with open BC.

The RSOC leads to a very rich magnetic landscape. Let us start by examining the results for $\chi(\mathbf{k})$, in the density- λ_{SO}/t_0 plane, and various values of J . In figure 1 we show the modulus of the peak of $\chi(\mathbf{k})$, $|\mathbf{k}_{peak}|$, which essentially describes the proximity to the FM state ($|\mathbf{k}_{peak}| = 0$), or to the AFM state ($|\mathbf{k}_{peak}| = 1$), its maximum value (in units of $\sqrt{2}\pi$) for the 8×8 cluster with open boundary conditions (BC).

For $J = 0$ (leftmost panel) and $\lambda_{SO} = 0$ there is a neat crossover from $\mathbf{k}_{peak} = (0, 0)$ to $\mathbf{k}_{peak} = (\pi, \pi)$ states at $\nu \approx 0.8$, consistently with previous studies. In the $\nu \gtrsim 0.8$ region, the behavior has been explained as a phase separated AFM-FM state [16] which we discuss below. As λ_{SO}/t_0 is increased, the peak of $\chi(\mathbf{k})$ departs from both FM and AFM states but remain close to them in the low and high electron density regions respectively, up to $\lambda_{SO}/t_0 \sim 2$. It is interesting to note that for very large relative values of the RSOC, $\lambda_{SO}/t_0 \gtrsim 4$ the situation is reversed, that is, the low (high) density region holds now a AFM (FM) state. As J is turned on, the region of FM is further shrunk, and the region with AFM order is extended to lower ν . Moreover, a new AFM region appears near $\nu = 0$. The region of FM order is suppressed by increasing λ_{SO}/t_0 similarly to what happens at $J = 0$.

3.2. Transport properties

The Drude weight D is calculated from the optical conductivity and the f-sum rule as:

$$\frac{D}{2\pi} = -\frac{\langle H_{0,x} \rangle}{2L} - \frac{1}{L} \sum_{n \neq 0} \frac{|\langle \Psi_n | j | \Psi_0 \rangle|^2}{E_n - E_0} \quad (2)$$

where $K_x \equiv -\langle H_{0,x} \rangle$ is the total kinetic energy of electrons along the x -direction [29].

The kinetic energy associated with the RSOC along the x direction, $K_{SO,x} = -\langle H_{0,SO,x} \rangle$ per site, and the total Drude peak, D , are shown in figure 2 for various values of λ_{SO}/t_0 and J . These results were obtained after averaging over periodic BC and “strip” BC (open along the y -direction and periodic along the x -direction), and in the later case we impose a phase in the electron wave-function or “twist”, $\Phi = 0, \pi/2$ and π in the appropriate units [21].

$K_{SO,x}/N$ shows an expected increase with both λ_{SO}/t_0 and J , in the later case due to suppression of FM order, which is unfavourable for RSOC (figure 2(a)). On the other hand, the Drude peak, within the dispersion of the data corresponding to different BC, is suppressed by increasing RSOC in a monotonous way, for $J \geq 0$ (figure 2(b,c)). For $J = 0$ and densities larger than $\nu \sim 0.75$, the Drude peak starts to decrease in a rather abrupt fashion (figure 2(b)). It has been noticed [16, 18, 21] that this suppression could be related to the Fermi level moving from

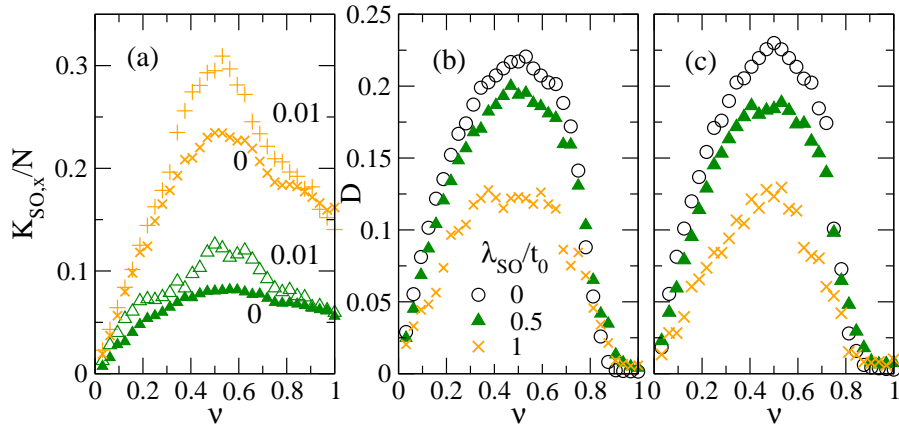


Figure 2. (a) Kinetic energy associated with the RSOC along the x direction, for two values of J as indicated in the plot. Total Drude peak for various values of λ_{SO}/t_0 and $J = 0$ (b) and $J = 0.01$ (c). Results for the 8×8 cluster averaged over periodic and twisted BC.

the bulk of the conduction band towards its high energy edge as ν is increased from $\nu \sim 0.75$, forming a pseudogap. Now, as J is increased, D starts to be suppressed at lower densities, as illustrated in figure 2(c) for $J = 0.01$, which is consistent with the reduction of the FM region shown in figure 1. At the same time another suppression of the Drude peak can be observed close to $\nu = 0$ where the FM order is also replaced by an AFM one by a positive J .

3.3. Phase separation

As emphasized in many previous studies on FKLM [16, 19], the behavior of magnetic and transport properties in the high density region can be understood by the presence of a phase separated state between AFM and FM orders. These two orders correspond to different stable electron fillings, one smaller than ~ 0.75 and the other equal to 1. The electron filling stability is determined by computing the so-called Maxwell construction.

Results for the 8×8 cluster with open BC are shown in figure 3(a) for $J = 0$ and various values of λ_{SO}/t_0 . For $\lambda_{SO} = 0$, that is, for the pure FKLM, we recover the well-known PS [16, 19] which extends between densities $\nu = 0.72$ and 1. As λ_{SO}/t_0 is increased such PS state is gradually suppressed, for example for $\lambda_{SO}/t_0 = 1$, the largest PS state extends between $\nu = 0.82$ and 0.94. This PS region is further reduced by increasing λ_{SO}/t_0 . As J is increased, first to 0.025 and then to 0.05 (figure 3(b) and (c) respectively) it can be seen that the PS region close to half-filling, for $\lambda_{SO} = 0$, extends to lower densities reaching $\nu = 0.6$ for $J = 0.05$. As λ_{SO}/t_0 is increased, this tendency to PS is suppressed. This behavior can be understood by the fact that the AFM effective exchange, which provides the attractive force leading to PS, is weakened and replaced by an effective stripe order with momentum close to (π, π) [21]. In addition, it should be noticed that close to $\nu = 0$, $\lambda_{SO} = 0$, another PS state appears for finite J , as originally reported in Ref. [17] for the FKLM. Similarly to what happens for high densities, the RSOC suppresses this PS state by the same mechanism discussed above. The PS region between $\nu = 0.14$ and $\nu = 0.42$ for $J = 0.05$ is explained by the fact that the two striped quasi-AFM states at the ends of this interval have lower energies than the FM states inside it. Then, the PS in this region is suppressed by the RSOC by raising the energies of the end AFM states.

4. Conclusions

In this work we have analyzed the interplay between the Rashba coupling on one side, and the hopping and Hund couplings that characterize the FKLM on the other. Near quarter-filling, the RSOC moves the system away from the ferromagnetic metallic state that is present in the pure

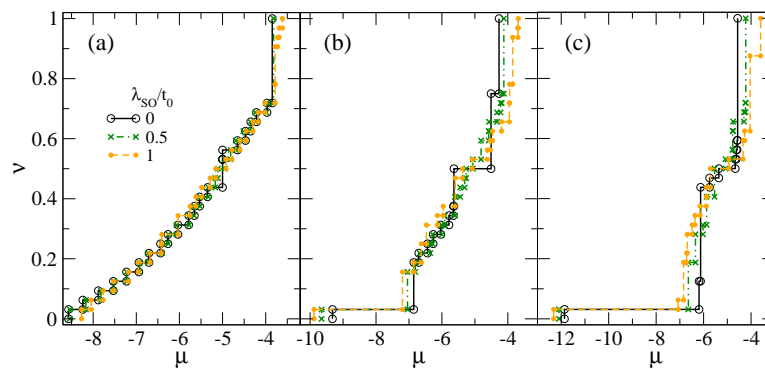


Figure 3. Density-chemical potential stability diagram for various values of λ_{SO}/t_0 , and $J = 0$ (a), 0.025 (b), and 0.05 (c). Results for the 8×8 cluster with open BC.

FKLM, leading to a rich variety of magnetic states and to a loss of conductivity. These effects are enhanced in the presence of a $J > 0$. Near half-filling, on the other hand, the mechanism that favours an AFM order in the pure FKLM is no longer fully acting in the presence of the RSOC, and the system moves away from this order. As a consequence the presence of phase separation between AFM and FM regions in the FKLM is suppressed by the RSOC. A similar effect is observed near the empty band where in the presence of $J > 0$ a new AFM phase appears.

5. References

- [1] Hwang H Y, Iwasa Y, Kawasaki M, Keimer B, Nagaosa N and Tokura Y 2012 *Nature Mater.* **11** 103
- [2] Rashba E I 1960 *Sov. Phys. Solid State* **2** 1109
- [3] Bychkov Y A and Rashba E I 1984 *JETP Lett.* **39** 78
- [4] R. Winkler 2003 *Spin-orbit Coupling Effects in Two-Dimensional Electron and Hole Systems* (Berlin: Springer)
- [5] D'yakonov M I and Perel V I 1971 *Sov. Phys. JETP* **33** 1053
- [6] Hirsch J E 1999 *Phys. Rev. Lett.* **83** 1834
- [7] Wolf S A, Awschalom D D, Buhrman R A, Daughton J M, von Molnar S, Roukes M L, Chtchelkanova A Y and Treger D M 2001 *Science* **294** 1488
- [8] Cavaglia A D, Gabay M, Gariglio S, Reyren N, Cancellieri C and Triscone J M 2010 *Phys. Rev. Lett.* **104** 126803
- [9] Caprara S, Peronaci F and Grilli M 2012 *Phys. Rev. Lett.* **109** 196401
- [10] Solov'yev I V 2011 *Phys. Rev. B* **83** 054404
- [11] Nakamura H, Koga T and Kimura T 2012 *Phys. Rev. Lett.* **108** 206601
- [12] Zener C 1951 *Phys. Rev.* **81** 440
- [13] Anderson P W and Hasegawa H 1955 *Phys. Rev.* **100** 675
- [14] de Gennes P G 1960 *Phys. Rev.* **118** 141
- [15] Riera J, Hallberg K and Dagotto E 1997 *Phys. Rev. Lett.* **79** 713
- [16] Dagotto E 2002 *Nanoscale Phase Separation in Manganites* (Heidelberg: Springer-Verlag)
- [17] Yunoki S, Hu J, Malvezzi A L, Moreo A, Furukawa N and Dagotto E 1998 *Phys. Rev. Lett.* **80** 845
- [18] Moreo A, Yunoki S and Dagotto E 1999 *Phys. Rev. Lett.* **83** 2773
- [19] Dagotto E, Hotta T and Moreo A 2001 *Phys. Rep.* **344** 153
- [20] Santos C and Nolting W 2002 *Phys. Rev. B* **65** 144419
- [21] Meza G A and Riera J A 2014 Magnetic and transport signatures of Rashba spin-orbit coupling on the ferromagnetic Kondo lattice model in two dimensions *Preprint arXiv:1405.1240*
- [22] Khalsa G, Lee B and MacDonald A H 2013 *Phys. Rev. B* **88** 041302
- [23] Bucheli D, Grilli M, Peronaci F, Seibold G and S. Caprara 2014 *Phys. Rev. B* **89** 195448
- [24] Shanavas K V and Satpathy S 2014 *Phys. Rev. Lett.* **112** 086802
- [25] Riera J A 2013 *Phys. Rev. B* **88** 045102
- [26] Pareek T P and Bruno P 2002 *Phys. Rev. B* **65** 241305
- [27] Duane S, Kennedy A D, Pendleton B J and Roweth D 1987 *Phys. Lett. B* **195** 216
- [28] Kennett M P, Berciu M and Bhatt R N 2002 *Phys. Rev. B* **66** 045207
- [29] Fye R M, Martins M J, Scalapino D J, Wagner J and Hanke W 1991 *Phys. Rev. B* **44** 6909